NPS-51MR72121A

NAVAL POSTGRADUATE SCHOOL

Monterey, California

DESCRIPTION OF A RADIATION PACKAGE
FOR THE
NAVAL POSTGRADUATE SCHOOL GENERAL CIRCULATION MODEL

by

Frank L. Martin

1 December 1972

NAVAL POSTGRADUATE SCHOOL
Monterey, California

Rear Admiral M. B. Freeman
Superintendent

M. U. Clauser
Provost

ABSTRACT

A method has been devised for integrating the pressure-scaled water-vapor and CO_2 absorber masses from the surface to the σ - levels used for prediction in the Naval Postgraduate School primitive equation model. Using empirical expressions for atmospheric absorptivity, scattering-reflectivity, cloud-reflectivity and earth-surface reflectivity, the useful solar insolations absorbed at earth and in the key atmospheric layers above the earth have been formulated. The terrestrial cooling effect at earth and in these same key atmospheric layers have also been formulated using recently published emissivities for the joint effects of water vapor and CO_2. As a result, the radiative heating (cooling) at key levels may be ascertained for input into the atmospheric thermodynamic equation. In addition, application of atmospheric boundary-layer modelling permits determination of the surface-layer turbulent transports (in the vertical) of sensible and latent heat at the earth's surface. These turbulent transports act in such a way as to provide a heat balance at the earth's surface.

NPS-51MR72121A

Table of Contents

1. Introduction

The radiation package described here is primarily an outgrowth of that used in the UCLA general circulation model (Gates et al. 1971), although some innovations from the corresponding model of NCAR (Oliger et al. 1970) and of the Geophysical Fluid Dynamical Laboratory (Manabe & Strickler 1964) have also been introduced.

The description here of the radiation package and its bearing upon the heat-budget of the earth and atmosphere is similar to that in use by Fleet Numerical Weather Central (Kesel & Winninghoff 1972) in application to the FNWC primitive-equation (P.E.) forecast model. The most obvious similarities are in the identical use of the same five σ-levels (with $\sigma = p/\pi$) for purposes of data-input, and also of similar criteria for the occurrence of a one-layer cloud deck. The main difference in the present from that of the FNWC model lies in the inclusion of water-vapor and CO_2 reduced optical masses in the σ-layer 0.4 to 0.2. This inclusion is made possible by a realistic method of extrapolation of the water-vapor specific humidity to levels above σ=0.4(see Appendix A). A more clearly defined system of integrations for the computation of net flux of terrestrial radiation is employed in this study (compared to that of FNWC) by means of new empirical absorptivities of water vapor and CO_2 (Sasamori, 1968).

The vertical-structure parameters needed to specify the properties of the radiating-absorbing model atmosphere sounding are given in Section 2. The solar-radiation package is described in terms of the model in Section 3, and the terrestrial radiation package is developed in Section 4.

2. The radiative vertical-structure parameters.

(a) Computation of absorber masses.

The five-layer model of Fig. 1 is similar to that in use in the FNWC primitive equation model. Since the half-layer σ - levels, denoted by the

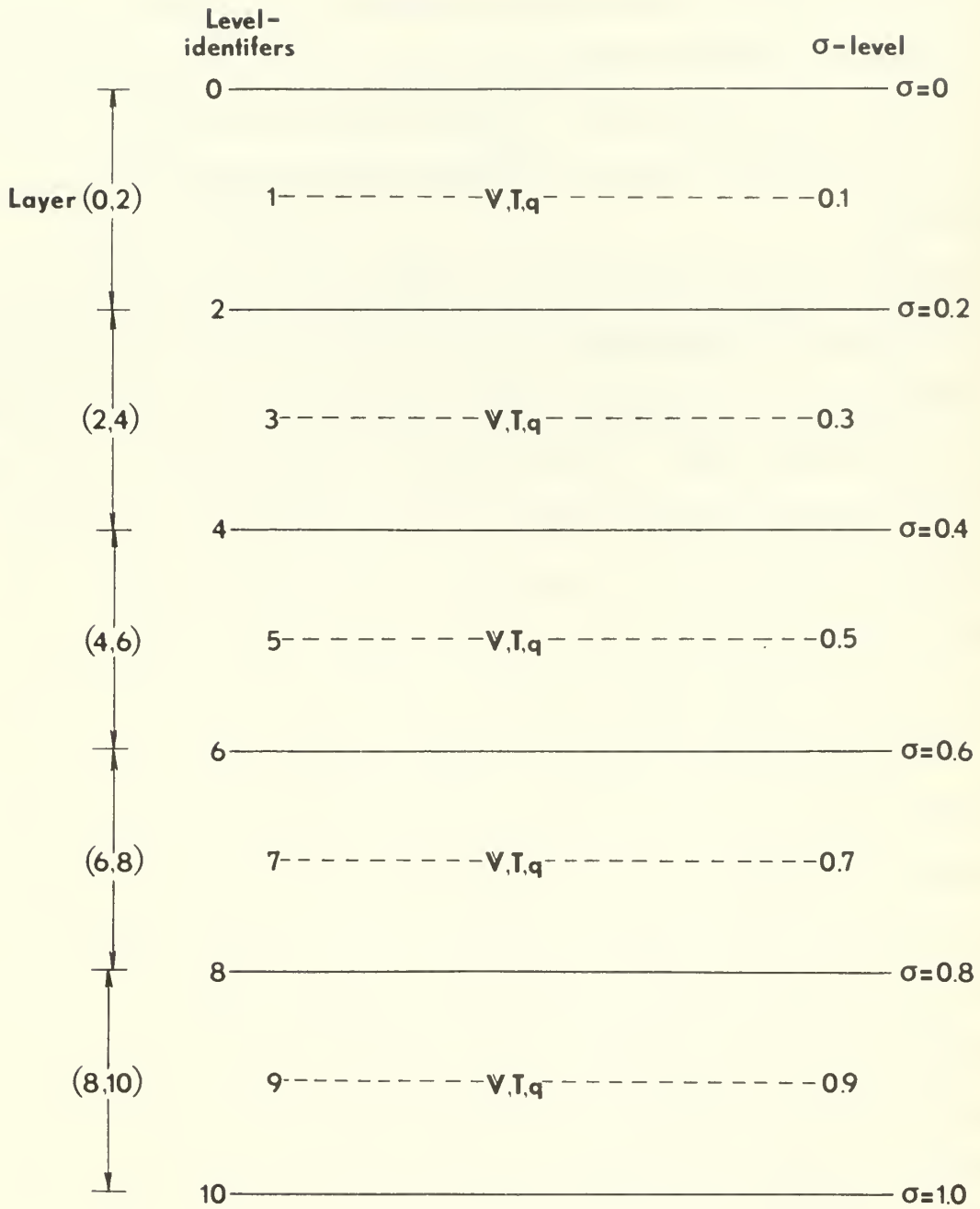

Fig. 1. Definition of the water vapor and CO_2 absorber mass parameters in the model. Moisture and temperature parameters are introduced at the odd-levels 10.0σ as in the analysis scheme. Levels are identified by their values on the 10.0σ scale, while layers are identified by their level boundary indices [e.g. (8,10)], in parentheses.

dashed lines are the primary levels for data-analysis of W, T, and q (= mixing ratio), there are a total of 10 levels important for radiational computations in the model. This happens because for each of the five levels where q is known, it is possible to determine the pressure-scaled water vapor absorbed mass $\Delta U(2k-1)$ and (similarly that of CO_2, $\Delta C(2k-1)$),associated with the center of each of the indicated five odd numbered levels. The appropriate formulas are

$$\Delta U(2k-1) = \frac{q_{2k-1}\,\Delta p}{g}\left(\frac{p_{2k-1}}{p_o}\right)^{.72} \qquad (2\text{-}1)$$

for water-vapor absorber mass in the layer 2k-2 to 2k. Here $\Delta p = .2\pi$ is a constant of the analysis scheme, and q_{2k-1} is the mean value of the water vapor mixing ratio centered in the layer (2k-2, 2k). The pressure-ratio factor $(p_{2k-1}/p_o)^{0.72}$ is the proposed scaling factor for collisional line-broadening, after Moller (1964). This formulation due to Moller, disposes of the necessity of temperature scaling in the usual Lorentz line-broadening formula (c.f., Danard, 1969), where the pressure-ratio scaling is linear and a temperature-ratio scaling is accomplished by $\left(\frac{T}{T_o}\right)^{-.5}$ times the mass within a layer.

For CO_2, Moller also proposes pressure-scaling similar in form to (2-1) but with a pressure-ratio exponent of 0.65. For simplicity a single pressure exponent of .72 will be adopted for both water-vapor and CO_2 absorber masses. Thus the layer-reduced absorber mass of CO_2 in N.T.P cm per cm^2 column is

$$\Delta C(2k-1) = 3.14 \times 10^{-4}\,\frac{\Delta p}{g\rho_o}\left(\frac{p_{2k-1}}{p_o}\right)^{0.72} \qquad (2\text{-}2)$$

In both Eqs. 2-1, 2-2 the subscript "o" denotes an N.T.P condition, e.g., p_o = 1013.25 mb, and ρ_o is the standard density at pressure $p = p_o$ and $T_o = 273.16^oK$.

For computation of radiative transfer, the total absorber mass (properly pressure-scaled) above a designated pressure level is needed. For our purpose here, it is most convenient to sum all absorber masses relative to the earth's surface, where 2k = 10. Thus the reduced absorber masses of Eqs. 2-1, 2-2 when applied to the layer (8, 10) become

$$\Delta U(9) \equiv U_{8,10} = \frac{q_9}{g} \Delta p \left(\frac{p_9}{p_o}\right)^{.72}$$

$$\Delta C(9) \equiv C_{8,10} = \frac{3.14 \times 10^{-4} \Delta p}{g\rho_o} \left(\frac{p_9}{p_o}\right)^{.72} \qquad (2\text{-}3)$$

The dual notation of (2-3) suggests the further procedure to be followed for incrementing absorber mass over specified layers in the atmosphere. The notation of (2-4)indicates the procedure for incrementation of mass adopted

$$U_{6,10} = U_{8,10} + U_{6,8}$$

$$C_{6,10} = C_{8,10} + C_{6,8} \qquad (2\text{-}4)$$

Here the method involves incrementing absorber mass only upward over successive layers in the five-layer atmosphere. The full atmospheric depth of absorber mass is likewise denoted by the symbolism

$$U_{0,10} = \sum_{k=5}^{o} U_{2k-2,2k}$$

$$C_{0,10} = \sum_{k=5}^{o} C_{2k-2,2k} \qquad (2\text{-}5)$$

where each term $U_{2k-2,2k}$ is similar in form to $U_{8,10}$, with the subscript 9 replaced by 2k-1.

Since it is understood that the integration of absorber-mass proceeds only from the surface upward, the second subscript "10" in (2-5) will be deleted. In line with these concepts, the following table summarizes the parameters (and their elevations) needed at each gridpoint to perform a radiation calculation.

Table 1. Notation for the distribution of radiative properties at even levels over gridpoints in the five-layer model.

$\sigma = p/\pi$	1.0	0.8	0.6	0.4	0.2	0.0
10σ	10.	8.	6.	4.	2.	0.
T_σ	$T_{10} \approx T_S$	T_8	T_6	T_4	T_2	T_0
U_σ	$U_{10} = 0$	U_8	U_6	U_4	U_2	U_0
C_σ	$C_{10} = 0$	C_8	C_6	C_4	C_2	C_0

Since the temperature and humidity analyses are carried along only at the odd levels σ =.9, .7, .5, .3, .1, it is generally necessary to extrapolate a temperature at the surface, T_{10}, using

$$T_{10} \approx T_S = .5(3T_9 - T_7) \qquad (2\text{-}6)$$

The temperatures at the other even-subscripted levels are available by linear interpolation between temperatures at odd-levels of 10σ. In general, no effective temperature at level "0" is available, and in fact the topmost available temperature analysis gives T_1, which will in general[1] be taken

[1] This will continue to be the case unless stratospheric temperature- and moisture-modelling are undertaken in future. Stratospheric modelling should be highly correlated with tropospheric features below.

as the effective temperature of the topmost absorber-mass increments of water vapor and CO_2 (U_0 and C_0), respectively.

2(b) Vertical extrapolation of the water-vapor mass to upper levels.

Smith (1966) has shown the existence of a strong correlation between q(p) and the surface value q_{10} through the extrapolative formula

$$\frac{q(p)}{q_{10}} = \left(\frac{p}{p_{10}}\right)^{\lambda} \qquad (2\text{-}7$$

Here λ is determined from the water-vapor sounding. In connection with the present study, the Northern Hemisphere soundings tabulated by London (1957) have been tested[2] to obtain a best-fit technique between ln q and ln p so that an equation of form

$$\frac{q(p)}{q_5} = \left(\frac{p}{p_5}\right)^{\lambda} \qquad (2\text{-}8)$$

might be obtained. The values of q(p) corresponding to σ = 0.1, .3, .5, .7, .9 were used to solve for the profile-parameter λ, which varied with latitude and season. The correlation coefficient which related ln q to ln p was determined with such high precision that use of (2-8) for extrapolation to σ = 0.1 was considered feasible when q(p) was available only at the levels p = 0.3, .5, .7, .9.

With q(1) known, the scaled absorber-mass U_2 modeled after $U_{8,10}$ of Eq. 2-3 was formulated for use in the model. In some cases values of q_3 will also be missing but such values are subject to retrieval from Eq. 2-8 using the mixing ratio values from $\sigma \geq 0.5$.

The procedure of water-vapor extrapolation to at least $\sigma \leqq .3$ should be considered a part of the model presented here with the relevant analysis

---

[2]By LT. R. J. Plante in his 1972-73 Master's thesis.

routine attached as a subprogram. The values of U_2 are quite small, but the transmissivities in the terrestrial spectrum are appreciable in any case.

2(c) Criterion for the existence of clouds at gridpoints.

In both the solar and terrestrial radiative transfer problems, it is essential to know the fractional cloud-cover CL at each gridpoint. This model, like that of FNWC, permits only a single cloud layer to form. The criterion for the amount CL of cloud-cover in existence at any gridpoint is given by Smagorinsky's (1960) algorithm (applicable at approximately 700 mb):

$$CL = 2.0 \left(\frac{e}{e_s} \right)_{\sigma=.7} - 0.7 \qquad (2\text{-}9)$$

Thus at every gridpoint there is a cloud-covered area CL of fractional amount $0 \leq CL \leq 1.0$, and a clear-area fraction $0 \leq 1 - CL \leq 1.0$.

When the fractional cloud-cover CL exists, the cloud is assumed to extend everywhere within the grid area square between $\sigma = .8$ to $\sigma = 0.4$.

The occurrence of $CL > 0$ of cloud amount profoundly affects the treatment of both the solar (Sec. 3) and terrestrial (Sec. 4) radiative transfer problems.

An improved cloud model permitting the introduction of a two-layer cloud system both of which fulfill Smagorinsky-type requirements is envisaged for future model development. Such improvements would follow a procedure somewhat similar to that of Oliger et al. (1970). This refined radiative cloud treatment would permit CL_1 of intermediate cloud between $\sigma=.8$ and $\sigma=.6$, and CL_2 of high cloud between $\sigma=.4$ and $\sigma=.2$. In the model of Oliger et al., the high-cloud layer is ascribed a solar transmissivity (or alternatively, a reflectivity) intermediate between moist air and a

mid-level cloud deck. Moreover, the distribution of the upper level cloud elements is assumed to overlap the lower-level ones in a random fashion.

2(d) Integrated absorber-mass formulas

If the result of (2-2) is summed from $p(2k) = (.2k)p_o$ to $p = p_o$ using straightforward integration, one obtains

$$C(2k) = 3.14 \times 10^{-4} \frac{p_o}{g\rho_o} \int_{(.2k)p_o}^{p=p_o} \left(\frac{p}{p_o}\right)^{.72} \frac{\Delta p}{p_o}$$

$$C(2k) = \frac{3.14 \times 10^{-4}}{1.72} H\left[1 - \left(\frac{p(2k)}{p_o}\right)^{1.72}\right] \quad (k=0,\ldots,5) \qquad (2\text{-}10)$$

where $H = 7.995 \times 10^5$ cm is the height of the homogeneous atmosphere. Since the surface pressure π may differ considerably from p_o, it is convenient to adapt Eq. 2-10 to the σ - levels of Fig. 1. This is easily done by setting the ratio

$$\frac{p(2k)}{p_o} = \frac{\pi}{p_o}\ \sigma\ (2k)$$

Thus C(2k) becomes

$$C(2k) = \frac{3.14 \times 10^{-4} H}{1.72} \left(\frac{\pi}{p_o}\right)^{1.72} \left[1 - \sigma_{2k}{}^{1.72}\right] \qquad (2\text{-}11)$$

where $\sigma = 0.0, 0.2, \ldots, 0.8, 1.0$ spans the 5-layers shown in Fig. 1. For water vapor, a similar integration of Eq. (2-1) over the layer (10,2k) gives the reduced absorber mass in this layer:

$$U(2k) = \left(\frac{\pi}{p_o}\right)^{1.72} \left(\frac{p_o}{1.72g}\right) \sum_{n=5}^{n=k\geq 1} \bar{q}_{2n-1} \left[\sigma_{2n}{}^{1.72} - \sigma_{2n-2}{}^{1.72}\right] \qquad (2\text{-}12)$$

In (2-12) $\bar{q}_{2n-1}$ is the variable mean mixing ratio of water vapor in the layer (2n-2,2n). The parameter $(\pi/p_o)^{1.72}$ is constant at a given gridpoint.

The computation of C(2k) and U(2k) then depends upon the values of $\sigma_{2k}^{1.72}$ at level 2k at each gridpoint. The following tabular values of $\sigma^{1.72}$ are useful in these computations

Level	2k	0	2	4	6	8	10
	σ_{2k}	0.0	.2	.4	.6	.8	1.0
	$\sigma_{2k}^{1.72}$	0.0	.06277	.20680	.41535	.68126	1.0

With U(2k) and C(2k) given by (2-12, 2-11), these mass parameters increase from the earth's surface upward.

3. The solar-radiative heating package.

(a) Partition of the solar spectrum at earth.

Following Joseph (1966), a solar constant of 2.00 ly min^{-1} is assumed, but is subject to 4% attenuation by oxygen and ozone absorption above the tropopause. Thus, an effective solar constant

$$S = 1.92 \text{ ly min}^{-1}$$

has been assumed entering the level $\sigma = 0.2$.

The effective insolation on any given Julian date D at level 2, Fig. 1, is then obtained from

$$F = S\left(\frac{r}{r_m}\right)^{-2} \cos\theta \qquad (3\text{-}1)$$

Here r/r_m is listed as a function of the date D in Smithsonian Table 169 (List, 1963). In addition, the zenith angle θ is available for any given time step (GMT), at latitude φ and longitude λ, using a subroutine of the FNWC radiation package (Kesel and Winninghoff, 1972, Appendix B).

Joseph (1966) has devised a computationally simple partition of the solar insolation into the part

$$F_A = 0.349 \text{ F.}$$

subject to water-vapor absorption but not to Rayleigh scattering in the atmosphere. The remaining insolation of the partition, denoted as

$$F_S = 0.651 \text{ F}$$

is subject only to Rayleigh scattering, but not to absorption in a <u>clear</u>, <u>moist</u> atmosphere. The presence of cloud-decks introduce cloud-reflectivities, however, in both the F_A and F_S solar-energy partitions. In any case, the F_S-energy comprises all wavelengths $\lambda \leq 0.9\ \mu$ m since here water-vapor absorption is negligible, while the F_A-category comprises solar

wavelengths $\lambda \geq 0.9\ \mu$ m where absorption by water vapor and CO_2 bands in the near infrared is the dominant attenuation process acting on the solar beam. In summary, the partition just devised gives rise to the parts

$$F_A = 0.349S \left(\frac{r}{r_m}\right)^{-2} \cos\theta \qquad (3\text{-}2)$$

$$F_S = 0.651S \left(\frac{r}{r_m}\right)^{-2} \cos\theta \qquad (3\text{-}3)$$

The component (3-2) contributes to atmospheric heating in any vertical column whenever $\cos\theta > 0$. The component (3-3) contributes only to earth-surface insolation, after scattering and reflective attenuations in the column above earth are considered (and when $\cos\theta > 0$).

In some climatological and general circulation investigations, e.g. Manabe and Strickler (1964), it has been found useful to compute the time-mean $\cos\theta$ for use in (3-2, 3-3) for the particular date under consideration. The following table, after Manabe and Möller (1961) lists daily mean values[3] of $\cos\theta$ as a function of latitude and time of the year. In addition, Table 2 lists the duration of the day in hours for these same arguments.

TABLE 2. The seasonal and latitudinal distributions of the length of the daytime given in parts of 24 hours and those of the weighted mean values of $\cos\theta$.

^{o}Lat.	Fractional length daytime				Weighted mean $\overline{\cos\theta}$			
	Apr.	July	Oct.	Jan.	Apr.	July	Oct.	Jan.
5	.508	.517	.500	.496	.625	.587	.614	.591
15	.521	.537	.492	.471	.618	.601	.579	.549
25	.533	.562	.483	.450	.599	.593	.524	.474
35	.546	.596	.471	.421	.558	.567	.458	.393
45	.562	.637	.454	.362	.501	.521	.379	.317
55	.596	.708	.437	.321	.423	.453	.282	.203
65	.629	.837	.404	.208	.345	.369	.176	.106
75	.750	1.000	.329	----	.241	.311	.071	----
85	1.000	1.000	----	----	.168	.318	----	----

[3] $\overline{\sec\theta}$ is very nearly equal to the reciprocal of $\overline{\cos\theta}$.

3(b) Disposition of F_S-insolation

A. Clear-sky F_S-insolation

Joseph (1966), found that the Rayleigh-scattering reflection values at sea level (after Coulson, 1959) could be fitted by least squares. The result was a best-fit regression of form

$$\alpha_s(\pi,\theta) = .085 + .25074 \log \left(\frac{\pi}{p_o} \sec \theta\right) \tag{3-4}$$

where π is the surface pressure and $p_o = 1013.25$ mb. The value of α_s is constrained never to exceed an upper limit of 0.99 even for large sec θ.

3(b)B. Earth-surface albedo

Another reflective-type parameter to be considered is that of surface albedo α_g, assumed constant over bare land as $\alpha_g = 0.14$ (except over deserts), but variable with respect to cos θ over the ocean:

$$\alpha_g(SEA) = MAX\left\{.06,\ .06 + .54(.7 - \cos\theta)\right\} \tag{3-5}$$

The value of α_g in the Sahara-Arabian desert is also considered a function of cos θ through

$$\alpha_g(DES) = .8 - .6 \cos\theta \tag{3-6}$$

The gridpoints which lie in these deserts are easily located in the FNWC model as corresponding to $I \geq 45$ and latitude $\varphi \leq$ arc sin .57. Also within the northern snowline (determined from monthly climatological surface temperatures $\bar{T}_{ij} \leq -3^oC$), α_g is obtained from the empirical result (Posey and Clapp, 1964):

$$\alpha_g(SNOW) = 0.4\left\{1.0 + \frac{(C_{LAT} - 5.)^2}{(C_{LAT} - 45.)^2 + (C_{LAT} - 5.)^2}\right\} \tag{3-7}$$

Here C_{LAT} is the number of latitude degrees poleward of the mean northern snowline. A similar expression applies for the south-polar ice-snowline. These values of α_g have been drawn from either the Kesel-Winninghoff (1972) or Gates et al (1971) documentations, respectively.

At any clear-sky gridpoint, the F_S-insolation is subject to the Rayleigh sky reflectivity α_s given by (3.4), and the appropriate earth-surface reflectivity α_g. Considering the possibility of multiple reflections between earth and atmosphere, each of which diverts downward the fraction α_s of the earth-surface reflectance α_g, the retained insolation in the earth is I_{so} given by

$$I_{so}(10) = F_s(1-\alpha_s)[1 + \alpha_s\alpha_g + \ldots(\alpha_s\alpha_g)^n + \ldots](1 - \alpha_g)$$

or

$$I_{so}(10) = \frac{F_s(1 - \alpha_s)(1 - \alpha_g)}{1 - \alpha_s\alpha_g} \qquad (3\text{-}8)$$

3(b)C. Cloudy-sky insolation in the F_S-region

(i) In the cloud layer

We make use of the Rayleigh reflection coefficient α_s of (3-4) applied only over air above the cloud-top at $p = .4\pi$. Since the cloud layer is composed of large water droplets, it is subject primarily to Mie-type or diffuse back-scatter which gives rise to the cloud-reflectivity parameter R_C (approximately, $R_C \doteq 0.5$), and also to the downward scattering which ultimately must emerge through cloud-base at $p = 0.8\pi$.

The two sky reflectivity factors $\alpha_s(\frac{.4\pi}{p_o} \sec\theta)$ due to air-scattering and R_C due to cloud-reflectance, go on independently with some downward reflection following each cloud-to-sky reflectance. Hence, an effective air-cloud transmissivity through the cloud-top similar to that implied by

(3-8) applies for F_S-insolation penetrating the cloud-top:

$$F_{sC}(4)\downarrow = \frac{F_s[1 - \alpha_s\ (\frac{.4\pi}{p_o} \sec \theta)][1 - R_C]}{(1 - \alpha_s\ R_C)} \qquad (3\text{-}9a)$$

Since the cloud-penetrating insolation $F_{sC}(4)\downarrow$ is not subject to absorption within the cloud, but only to forward Mie-scattering, the fraction emerging as transmitted through the base is likely to have the mean slant-path for diffuse radiation, so that F_{sC} becomes

$$F_{sC}(8)\downarrow = \frac{F_s[1 - \alpha_s(\frac{.4\pi}{p_o} \sec \theta_D)][1 - R_C]}{[1 - \alpha_s\ R_C]} \qquad (3\text{-}9b)$$

Here $\sec \theta_D = 1.66$ has replaced $\sec \theta$ as in most cases of diffuse-sky slant paths (Katayama, 1966). Wherever α_s appears either in the numerator or in the denominator, the value of π in (3-4) has been replaced by $.4\pi$ and $\sec \theta$ by $\sec \theta_D = 1.66$. The value F_{sC} of (3-9b) then gives the transmitted diffuse beam entering the subcloud layer. In this layer, $F_{sC}\downarrow$ will be subject to further multiple reflections to be discussed below.

3(b)C. (ii) Partition of $F_{sC}(8)\downarrow$ in the subcloud layer.

The assumption is made here that Rayleigh scattering by air molecules occurs in the air-layer between $p = 0.8\pi$ to $p = 1.0\pi$. Furthermore, the mass of air involved in this layer is 0.2π, and the angle θ is still subject to the diffuse slant-path condition arc sec $\theta = 5/3$. As a result, the subcloud scatter-reflectivity α_s becomes, by analogy with Eq. 3-4:

$$\alpha_s(8\text{-}10) = .085 + .25074 \log (\frac{0.2\pi}{p_o}\ \frac{5}{3}) \qquad (3\text{-}10)$$

The diffuse beam $F_{sC}(8)\downarrow$ which first enters the subcloud layer is subjected to a sequence of reflections depicted schematically in Fig. 2. Consider the beam B_1G_1 associated with the first entry of $F_{sC}(8)\downarrow$ at point B_1 of the subcloud layer (Fig. 2). The fraction α_s is turned upward during the first transit and the fraction $(1 - \alpha_s)$ reaches the earth at G_1. In addition to α_s, the further fraction $\alpha_g(1 - \alpha_s)$ is also turned upward from the first entering beam B_1G_1 before earth-absorption occurs. The beam B_1G_1 therefore has been decomposed into the parts

$(1 - \alpha_s)(1 - \alpha_g)\ F_{sC}$ into earth at G_1

$[\alpha_s + \alpha_g(1 - \alpha_s)]F_{sC}$ starts along G_1-B_2

The latter part is assumed to reach the point B_2, where the subsequent multiplicative fraction R_C starts down from B_2 towards G_2. The intervening subcloud scattering layer reduces the transmission along B_2G_2 by the factor $(1 - \alpha_s)$; hence at G_2, we have the downcoming second diffuse beam insolation contribution

$$[\alpha_s + \alpha_g(1 - \alpha_s)] \cdot (1 - \alpha_s)\ R_C\ F_{sC}(8)\downarrow$$

with a further decomposition into the parts

$[\alpha_s + \alpha_g(1 - \alpha_s)](1 - \alpha_s)\ R_C\ \alpha_g\ F_{sC}$ --- reflected at G_2

$[\alpha_s + \alpha_g(1 - \alpha_s)](1 - \alpha_s)(1- \alpha_g)\ R_CF_{sC}$---absorbed at G_2

Continuation of this process of successive reflections between ground and cloudbase yields the final cumulative absorption at the earth, denoted as $I_{sC}(10)$

$$I_{sC}(10) = (1-\alpha_s)(1-\alpha_g)F_{sC}+[\alpha_s+\alpha_g(1-\alpha_s)](1-\alpha_s)(1-\alpha_g)R_CF_{sC}$$
$$+ [\alpha_s+\alpha_g(1-\alpha_s)](1-\alpha_s)^3(1-\alpha_g)R_C^2\ \alpha_g\ F_{sC}+.....+....,$$

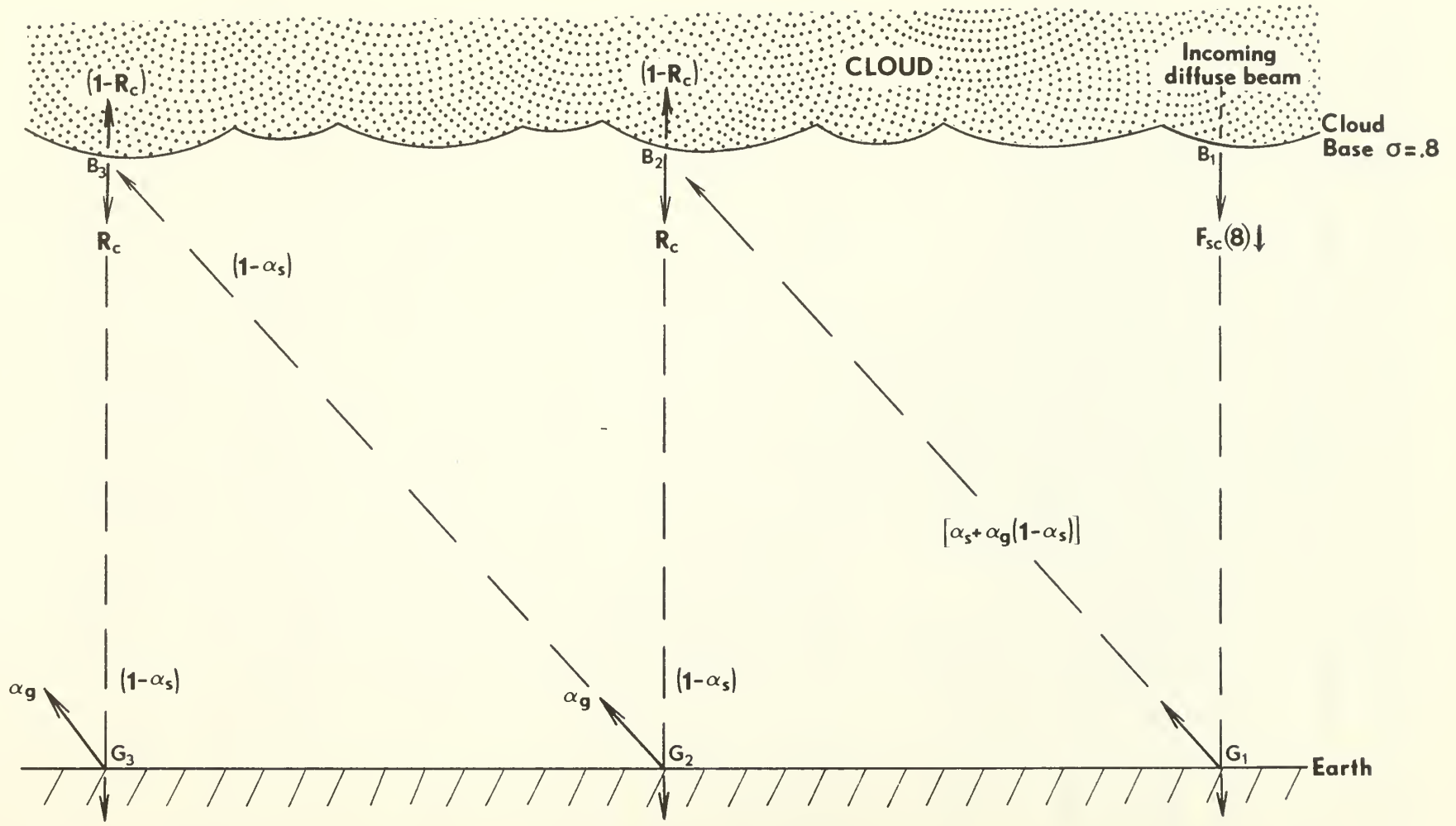

Fig. 2. Disposition of diffuse-sky solar insolation $F_{SC}(8)\downarrow$ penetrating into the sub-cloud layer. A sequence of multiple reflections applied to the beam in giving contributions to ground-penetration and cloud-penetrations (leakage) is schematically indicated.

and on through higher terms. Finally, upon simplification, one obtains

$$I_{sC}(10) = F_{sC\downarrow}(1-\alpha_s)(1-\alpha_g) + \frac{F_{sC\downarrow}[\alpha_s + \alpha_g(1-\alpha_s)](1-\alpha_s)(1-\alpha_g)R_C}{[1 - R_C(1-\alpha_s)^2\,\alpha_g]} \qquad (3\text{-}11)$$

In the above accounting, certain small atmospheric reflection terms from the subcloud layer to earth or to cloud have been ignored as small compared to the air-transmission factor $(1-\alpha_s)$.

It is to be stressed that $I_{sC}(10)$ given by Eq. 3-11 is the absorbed insolation at earth, resulting from the F_S-insolation of Eqs. 3-3 and 3-9b. The parameter α_s always arises as a modification of Eq. 3-4 depending upon the depth of the scattering layer. α_g and R_C are subject to variability depending upon the surface and cloud albedos, although $R_C \doteq 0.5$ is assumed as a first approximation. In the F_S-wavelengths no atmospheric absorption occurs. The weighted mean earth-surface absorption then becomes

$$I_s(10) = (1 - CL)I_{so} + CL\ I_{sC}(10) \qquad (3\text{-}12)$$

where I_{so} is given in (3-8), and $I_{sC}(10)$ in (3-11).

A related subject of some interest concerns the leakage back to space of the subcloud insolation (Eq. 3-9b) after upward cloud-transmittance.

Cloud-leakage. It is of interest to compute the solar-leakage through the cloud base subject to the approximation noted in the paragraph just below Eq. 3-11. Reference to Fig. 2 indicates that the sum total beam-transmittances at the cloud-base involve solar energy leaks of sequential amounts indicated by the following sum of terms:

$$F_{sC,B}\uparrow = F_{sC\downarrow}[\alpha_s + \alpha_g(1-\alpha_s)]\left\{(1-R_C) + R_C\alpha_g(1-\alpha_s)^2(1 - R_C) + (R_C\alpha_g)^2(1-\alpha_s)^4(1-R_C)+\ldots\right\}$$

or

$$F_{sC,B}\uparrow = F_{sC}[\alpha_s + \alpha_g(1-\alpha_s)](1-R_C)\left[\frac{1}{1-R_C\alpha_g(1-\alpha_s)^2}\right] \qquad (3\text{-}13)$$

Comparison of (3-13) with (3-11) indicates that the leakage is closer to the order of magnitude of the second (smaller) term of (3-11). Choosing $\alpha_s \approx 0.05$, and average values $\alpha_g = 0.14$, $R_C = 0.5$, indicates the leakage to be about $0.1\ F_{sC}(8)\downarrow$ or about 3% of the extraterrestrial insolation of Eq. 3-1. This leakage represents an additional component to be added to the planetary albedo in cloud-covered areas only. Again it is to be stressed that none of the F_S radiation is absorbed by the atmosphere in this model.

3.(c) Disposition of F_A-insolation

(A) Clear areas

Here absorption of the F_A-component of the insolation is considered. Use of the Manabe-Möller solar absorptivity[4] function $\underline{a}(u \sec\theta)$ in the form

$$a = .0946\ (U_{2,2k} \sec\theta)^{.303} \qquad (3\text{-}14)$$

will be used extensively in this discussion as well as in that of the cloudy-sky case discussed below. The form of Eq. 3-14 indicates that the absorption function $\underline{a}$ is applied over the corrected water vapor path between levels 2 and 2k (see Fig. 1) along the zenith-path of slant angle θ. Actually (3-14) is applicable to the entire solar energy F. Restricting absorption to the ratio 0.349F requires that the multiplicative constant

[4] The symbol $\underline{a}$ denotes the fractional absorptivity function, while A(2,2k) denotes the absorbed energy between levels 2 and 2k.

of (3-14) be adjusted to (.0946/0.349) = .271. Hence the absorbed insolation in the layer (2,6) becomes simply

$$A(2,6) = .271\ (U_{2,6}\ \sec\theta)^{.303} F_A \qquad (3\text{-}15)$$

Similarly, the absorbed insolation in the layer (2,10) is

$$A(2,10) = .271(U_{2,10}\ \sec\theta)^{.303} F_A \qquad (3\text{-}16)$$

The absorbed insolation in the layer (6,10) is then given by

$$A(6,10) = A(2,10) - A(2,6) \qquad (3\text{-}17)$$

Finally, the difference formed by subtracting A(2,10) from F_A gives the direct transmission of F_A-insolation to the earth's surface. This direct-transmission $[F_A - A(2,10)]$ is denoted by $F_A(10)$ and is partially reflected (the fraction α_g is applicable). The remainder $(1-\alpha_g)F_A(10)$ is absorbed at earth. The F_A-insolation absorbed at earth is given by

$$I_{A\odot}(10) = F_A[1-.271(U_{2,10}\sec\theta)^{.303}](1-\alpha_g) \qquad (3\text{-}18)$$

In the foregoing derivation, solar absorption was computed only below level 2 of Fig. 1, as a 4% stratospheric reduction of the solar beam was previously applied in the layer above level 2. Likewise no accounting of the terrestrial spectral absorption in this topmost layer will be made. This implies the assumption that the layer $\sigma \leq .2$ is in continual radiative heat balance at all gridpoints.

3(c).B. F_A-insolation; Cloudy-sky areas

In the layer (2,4), the Manabe-Möller absorption is employed in a manner similar to Eq. 3-15 apart from the differing water-vapor mass $U_{2,4}$:

$$A(2,4) = 0.271(U_{2,4}\sec\theta)^{.303} F_A \qquad (3\text{-}19)$$

The F_A-insolation at level 4 is therefore

$$F_A(4) = F_A[1 - .271(U_{2,4}\sec\theta)^{.303}] \qquad (3\text{-}20)$$

Of the energy $F_A(4)$, the fraction $1 - R_C$ is transmitted through the cloud top which interfaces at level 4. Hence the downward transmitted F_A-insolation through the cloud top is

$$F_A(4)\downarrow = F_A(1 - R_C)[1-.271(U_{2,4}\sec\theta)^{.303}] \tag{3-21}$$

Within the cloud layer, the water-vapor path in layer (4,6) is subject to the mean diffuse-path augmentation factor 5/3 (after Katayama, 1966). Thus the energy-absorption A(4,6) is given by

$$A(4,6) = F_A(4)\downarrow *.271[\tfrac{5}{3}(U_{4,6} + \frac{U_C}{2})]^{.303} \tag{3-22}$$

In (3-22), the water-vapor parameter U_C is the water-vapor mass equivalent of the cloud-droplet absorption. The determination of the parameter U_C which is spread vertically over the cloud-layer (4,8) is modeled after estimates of cloud-droplet absorptivity a_{CLD} [given by Korb et al.(1956)] and makes use of the modelling assumption

$$a_{CLD} = .271\left\{[\tfrac{5}{3}(U_{4,8} + U_C)]^{.303} - [\tfrac{5}{3}U_{4,8}]^{.303}\right\} \tag{3-23}$$

The method of computation of $U_C/U_{4,8}$ is detailed in Appendix C as a function of $U_{4,8}$ for the latitude bands 0-40, 40-65, 65-90.

With U_C known at each gridpoint, the following three computations of insolation are made

$$A(4,6) = F_A(4)\downarrow \left\{.271[\tfrac{5}{3}(U_{4,6} + \frac{U_C}{2})]^{.303}\right\} \tag{3-24}$$

$$A(6,10) = F_A(4)\downarrow \left\{.271[\tfrac{5}{3}(U_{4,10} + U_C)]^{.303} - [\tfrac{5}{3}(U_{4,6} + \frac{U_C}{2})]^{.303}\right\} \tag{3-25}$$

$$I_{gC}\downarrow = F_A(4)\downarrow \left\{1-0.271[\tfrac{5}{3}(U_{4,10} + U_C)]^{.303}\right\} \tag{3-26}$$

These three computations represent respectively (i) the absorbed insolation in the layer (4,6), (ii) the absorption in layer (6,10), and (iii) the transmission to the earth's surface. The last of these is subject to the multiplicative earth-absorption factor P (of form similar to Eq. 3-8)

$$P = (1 - \alpha_g)/(1 - \alpha_g R_C) \tag{3-27}$$

This factor P when multiplied by $I_{gC}^{\downarrow}$ of (3-26) gives the F_A-penetration of the earth's surface under cloudy skies.

In summary, the gridpoint absorption of F_A-energy in earth now becomes the cloud-weighted sum

$$I_A(10) = (CL)(P \text{ of } 3\text{-}27)(I_{gC} \text{ of } 3\text{-}26)+(1 - CL)(I_{A0} \text{ of } 3\text{-}18) \tag{3-28}$$

Similar cloud-weighted sums of absorption of F_A-energy should be formed for the layers (6,10) and (2,6). In the latter connection, it should be recalled that the F_A cloudy-sky result in layer (2,6) is made up of the two contributions (3-19), (3-22), the former of which has no cloud-reflectivity factor $(1 - R_C)$ since it pertains to A(2,4) only.

3(d) Summary of solar-heating effects

The results of Sections 3b, 3c are now combined to get a resultant insolational-absorption at earth. This is done by summing the two contributions $I_S(10)$ of Eq. 3-12 and $I_A(10)$ of (3-28).

Within the atmospheric layers (2,6), (6,10), only the F_A wavelengths contribute to absorption and therefore to temperature-change through

$$\frac{\partial T}{\partial t}(2,6) = \frac{A(2,6) \text{ cals/cm}^2\text{/hr}}{.4\pi(\frac{1000}{g})[C_p]} \tag{3-29}$$

$$\frac{\partial T}{\partial t}(6,10) = \frac{A(6,10)\ \text{cal/cm}^2\text{/hr}}{.4\pi(\frac{1000}{g})C_p} \qquad (3\text{-}30)$$

The first of these temperature-changes involves the cloud-weighted composite absorption rate formed from A(2,6) of (3-15) and from A(2,4), A(4-6) of Eqs (3-19,22). Similar weighted means are needed for A(6,10).

4. Formulation of net cooling rates by terrestrial radiation

(a) Clear-sky areas

It should be recalled that Table 1 contains the format of a "radiative" sounding having input data defined at the levels listed in Table 3.

Table 3. Levels and data used in the "radiative" soundings.

Levels	10	8	6	4	2	1	0
Temperature	$T_{10} \doteq T_S$	T_8	T_6	T_4	T_2	T_1	T_0
W.V.mass	$U_{10} = 0$	U_8	U_6	U_4	U_2	U_1	U_0
CO_2 mass	$C_{10} = 0$	C_8	C_6	C_4	C_2	C_1	C_0

The value of water-vapor reduced absorber-mass $U_{2k}(k = 5,....,0)$ was defined in Section 2(d), as was also the corresponding value of C_{2k}. These values have been incremented upward relative to the ground as indicated by Eqs. 2-12, 2-11, respectively. In these equations the notation U(2k) has been treated interchangeably with the more compact notation U_{2k} used here, and in the remainder of this section.

Consider the radiative temperature change in air. By the first law of thermodynamics, this is given by

$$\frac{\partial T}{\partial t} = - \frac{(F_6^* - F_{10}^*)}{0.4\pi \frac{1000}{g} C_p} \qquad (4\text{-}1)$$

for the layer (6,10). For the layer (2,6), the corresponding formula is given by

$$\frac{\partial T}{\partial t} = - \frac{(F_2^* - F_6^*)}{0.4\pi \frac{1000}{g} C_p} \qquad (4\text{-}2)$$

The numerators of (4-1), (4-2) which are contained within parentheses are understood to be flux-divergences from the atmospheric columns (6,10) and (2,6) over the gridpoint having the indicated "radiative" sounding.

Virtually all of radiation packages in the presently used large-scale circulation models in the United States [cf., Manabe and Strickler (1964), Oliger et al. (1970), Arakawa et al. (1969)] make use of Yamamoto's (1952) water vapor flux-emissivities as a basis for their radiative flux calculations. These absorptivities $\epsilon(U,T)$ as defined below are virtually independent of temperature in the normal range of temperatures ($300K \geq T \geq 220K$), but at temperatures $T \leq 220^{o}K$ the wave-averaged flux-emissivity function defined in (4-3) after Yamamoto (1952) and others, has the form

$$\epsilon(U,T < 220) = \frac{\int_{o}^{\infty} [1-\tau_{F\nu}(L_{\nu o}U)] \frac{dB_{\nu}}{dT} (T=220K)d\nu}{\int_{o}^{\infty} \frac{dB_{\nu}}{dT} (\nu,T)\, d\nu} \qquad (4\text{-}3)$$

It is seen that the numerator of (4-3) has its temperature-dependent terms fixed at 220K, while the denominator equals $4St^{*}T^{3}$ even when $T < 220K$. Thus (4-3) introduces a temperature-dependent flux-emissivity for temperatures $T < 220K$, reflecting the effect of increased absorptivity by the rotational band of atmospheric water-vapor which takes effect in view of Wien's law at these low temperatures. In the discussion which follows, the absorptivity will be restricted to be due to water-vapor alone, until the subject of CO_2 is specifically introduced. Although analytic functions

have been determined for $\epsilon(U,T)$ for both water vapor and CO_2, it is useful to examine schematic versions of the Yamamoto method of net flux calculations through key levels of the sounding (Table 3). Schematic net flux depictions are shown in Fig. 3 for the levels 10., 6., 2. in cases (A), (B), (C), respectively.

4a. (A) Net flux at level 10.

Sasamori (1968) has empirically recomputed $\epsilon(U)$ after Yamamoto's (1952) values for the temperature-independent part of atmospheric radiational soundings, schematic versions of which are shown in Fig. 3. The temperature-independent emissivity $\epsilon(U)$, after Sasamori (1968) is

$$\epsilon(U) = .240 \log_{10}(U + .010) + .622 \qquad (4\text{-}4)$$

in the temperature-independent region $T \geq 220K$. For $T < 220K$, Sasamori gives for the temperature-dependent emissivity

$$\bar{\epsilon}(U,T) = (8.34T^{.353\log_{10}U-.44})\, U^{-.03455\log_{10}U-.705} \qquad (4\text{-}5)$$

Here U represents the final U-value relative to the reference level considered to be level 10, so that

$$\bar{\epsilon}(U,T) = (8.34T^{.353\log_{10}U_o-.44})\, U_o^{-.03455\log_{10}U_o-.75} \qquad (4\text{-}6)$$

Corresponding to this value of U_o, a temperature-dependent $\bar{\epsilon}$-isopleth converges into the lower left corner of each panel of Fig. 3, i.e., $\bar{\epsilon} \to 1.0$ as $B(T=0)= 0$, where $B = \sigma T^4$ is the Stefan-Boltzmann flux.

The trapezoidal summation-rule gives a representation of the hatched (downward flux) area of Fig. 3A as

$$\begin{aligned} F_{\downarrow}(10) = .5 \Big\{ & \epsilon(8\text{-}10)(B_{10}-B_8) + [\epsilon(8\text{-}10)+ \epsilon(6\text{-}10)](B_8- B_6) \\ & + [\epsilon(6\text{-}10)+ \epsilon(4\text{-}10)](B_6-B_4)+[\epsilon(4\text{-}10)+ \epsilon(2\text{-}10)](B_4-B_2) \\ & + [\epsilon(1\text{-}10)+ \epsilon(2\text{-}10)](B_2-B_1)+ 2\int_{B=0}^{B(T_1)} \bar{\epsilon}(0\text{-}10,T)\,dB \Big\} \end{aligned} \qquad (4\text{-}7)$$

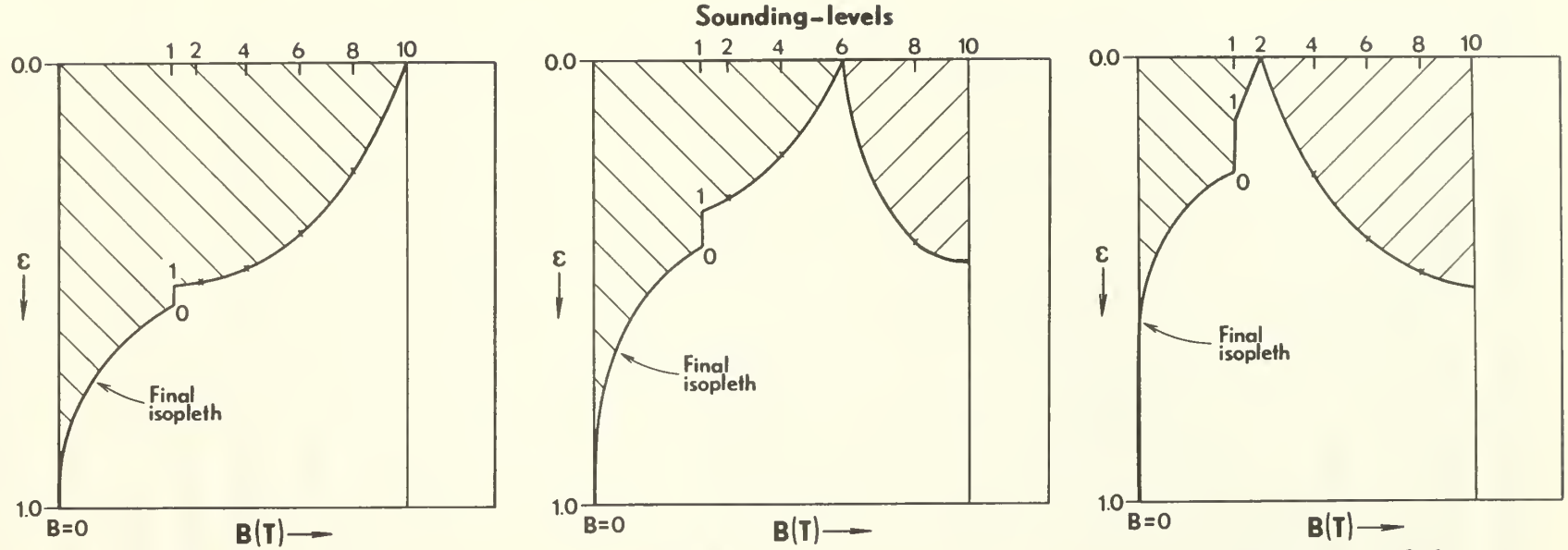

(A) F* at σ = 1.0 (B) F* at σ = .6 (C) F* at σ = 0.2

Fig. 3. Net water-vapor flux diagrams at sounding level (A) σ = 1.0; (B) σ = 0.6; (C) σ = 0.2 for clear-sky cases only. The desired integral is $St^*T_{10}^4$ minus the hatched areas bounded by the sounding curves in each case. The hatched areas in each case are computed by the trapezoidal rule applied to the integrations

$$\int_{B=0}^{B_{10}} \varepsilon dB$$

where $\bar{\epsilon}$ in the final term is the function of U,T listed in (4-5). The notation $\epsilon(8\text{-}10)$ denotes $\epsilon(U_8\text{-}U_{10})$ etc, while $B_{10} = St^*T_{10}^4$, $St = 5.67332 \times 10^{-9}$ cal cm^{-2} hr^{-1} $^oK^{-4}$ and so on for all of the other black-body fluxes (B_8, B_6, B_4, B_2, B_1, B_0), distributed along the sounding of Table 3.

Note that the final integral $\int \bar{\epsilon}\, dB$ of (4-6) may be evaluated by the integration

$$\int \bar{\epsilon}\, dB = 8.34\, U_{0,10}^{-.03455\log_{10}U_0-.705} \int_0^{T=T_1} T^{.3531\log_{10}U_0-.44}\, 4St^*T^3 dT$$

$$= St^*T_1^4 \left\{ 8.34 U_0^{-.03455\log U_0-.705} \cdot \frac{4T_1^{.3531\log U_0-.44}}{.3531\log_{10}U_0+356} \right\}$$

It finally follows that

$$\int_0^{B_1} \bar{\epsilon}\, dB = St^*T_1^4 * \bar{\epsilon}(U_0,T_1) * \frac{4}{.3531\log_{10}U_0+3.56} \qquad (4\text{-}8)$$

with $\bar{\epsilon}(U_0,T_1)$ defined in (4-5).

Hence F_{10}^* is given by

$$F_{10}^* = B_{10} - F_{\downarrow}(10) \qquad (4\text{-}9)$$

with the latter term given by Eq. 4-6, 4-7.

B. Net flux at level 6

In this case, the desired net flux is represented by $B(T_{10})$ minus the slant-hatched area above the sounding curves of Fig. 3B. Thus the result may be modeled after the results 4-6, and 4-7

$$F_6^* = B_{10} - .5 \left\{ \epsilon(6\text{-}8)(B_8-B_6) + [\epsilon(6\text{-}8) + \epsilon(6\text{-}10)](B_{10} - B_8) \right.$$
$$+ \epsilon(4\text{-}6)(B_6-B_4) + [\epsilon(4\text{-}6) + \epsilon(2\text{-}6)](B_4 - B_2)$$
$$+ [\epsilon(2\text{-}6) + \epsilon(1\text{-}6)](B_2 - B_1)$$
$$\left. + (St)T_1^4 * \bar{\epsilon}(U_{0,6},T_1) * \frac{8.0}{.353\ \log U_{0,6} + 3.56} \right\} \qquad (4\text{-}10)$$

Here $\bar{\epsilon}(U,T)$ is defined in (4-5) while $\epsilon(|U_{2k} - U_6|)$ is defined in (4-4).

C. Net flux at level 2

Fig. 3C is relevant for this computation. The net flux at level 2 may therefore be written as follows by analog with Eqs. 4-8, 4-6, 4-5, 4-4:

$$F_2^* = St^*T_{10}^4 - .5\{\epsilon(2\text{-}4)(B_4 - B_2) + [\epsilon(2\text{-}4) + \epsilon(2\text{-}6)](B_6 - B_4) + [\epsilon(2\text{-}6) + \epsilon(2\text{-}8)](B_8 - B_6) + [\epsilon(2\text{-}8) + \epsilon(2\text{-}10)](B_{10} - B_8) + \epsilon(102)(B_2 - B_1) + St^*T_1^{4*}\,\bar{\epsilon}(U_{0,2}T_1)^* \frac{8.0}{.353\ \log U_{0,2} + 3.56}\} \qquad (4\text{-}11)$$

where $B_k = St^*T_k^4$

With F_2^*, F_6^*, F_{10}^* formulated in terms of radiative-sounding parameters by Eqs. 4-7 and 4-9, 4-10 and 4-11 respectively, layer-mean temperature-change rates in $^oK(hr)^{-1}$ may now be calculated. Before this is done, however, it is convenient to introduce the modifications in F_2^*, F_6^*, F_{10}^* resulting from the inclusion of CO_2 flux-emission.

D. Inclusion of CO_2 absorber-mass in F^* calculations

The "area" integrals $\int_{U=0}^{U_N} \epsilon(U,T)\, dB$ depicted in Fig. 3 have been computed by integrating along a two-path sounding curve away from the reference level (Fig. 3A,B,C). When absorption is due both to water vapor and CO_2, the product-law of transmissivities must be employed. In doing this the transmissivity of the two absorbers acting jointly is expressed as

$$\tau_F(U,C) = \tau_F(U)\ \tau_F(C)$$

Then the flux-integral becomes

$$F\downarrow = \int_{U,C=0}^{U_N,C_N} [1-\tau_F(U)\tau_F(C)]dB = \int_{U=0,C=0}^{U_N,C_N} \{[1-\tau_F(U)] + \tau_F(U)\ \epsilon_F(C)\}\ dB \qquad (14\text{-}12)$$

"w.v.flux" "CO_2"

The first term on the right is the water-vapor flux computed using for example Eq. 4-7 and ignoring the emission by CO_2. The second-term, denoted "CO_2", represents the effective emission due to CO_2 not already counted in the water-vapor flux computation. The added emission is expressed schematically on the Yamamoto chart by an increase of emissivity at all points of the radiative soundings (except at the reference level points). Thus at any temperature T, the required joint-emissivity is obtained by replacing that due to water-vapor already computed, $\epsilon_W(U)$, by

$$\epsilon_{WC} \equiv \epsilon_W(U) + \Delta\epsilon_{WC}(U,C).$$

The last term includes the 15 μm band emitted flux of CO_2 which has not already been counted in emission by the rotational band of water vapor. Sasamori (1968) has computed this 15 μm band "overlap" region emissivity, and developed the empirical correction shown in (4-13, 4-14) below:

$$\Delta\epsilon_{W,C}(U_{2k}, C_{2k}) = \tau_W^{OVL}(U_{2k}) * \epsilon_C(C_{2k}) \qquad (4\text{-}13)$$

$$\Delta\epsilon_{WC}(2k) = .07262 \left\{1-.62556(U_{2k}+.286)^{.26}\right\} \left\{\log C_{2k} + 1.064\right\} \qquad (4\text{-}14)$$

Thus in considering the flux-modification for the inclusion of CO_2, one simply computes the added emissivity-values $\Delta\epsilon_{WC}$ of (4-14) at each sounding point. In the summation Eq. 4-7, for example, where $\epsilon(8\text{-}10)$ appeared, this term is simply replaced by the function

$$\epsilon_W(U_8 - U_{10}) + \Delta\epsilon_{WC}[(U_8 - U_{10}), (C_8 - C_{10})]$$

where the function $\Delta\epsilon_{WC}$ term uses the simultaneous values $U_8 - U_{10}$ and $C_8 - C_{10}$ stored from the radiative sounding. The 15 μm effective emissivity $\Delta\epsilon_{WC}$ of Eq 4-14 is considered to be temperature-independent (Sasamori, 1968)

in the range $T \leq T_1 \leq 220K$, in which range the water-vapor emissivity ϵ_W was temperature-averaged. Hence in Eq. 4-7, the final term of $F^{\downarrow}(10)$ becomes

$$St * T_1^4 [\bar{\epsilon}_W(U_0, T_1)(\frac{8.}{.353 \log_{10} U_0 + 3.56}) + \epsilon_{WC} \text{ of (4-14)}] \qquad (4\text{-}15)$$

where $\Delta\epsilon_{WC}$ in the last term of the bracket in (4-15) involves substitution of U_0, C_0 for U,C in (4-14).

With the revised formulations for F_2^*, F_6^*, F_{10}^* it is appropriate to compute the flux divergences in the layers (2,6), (6,10) and finally

$$F_{10}^* = B_{10} - F_{WC}(10)^{\downarrow} \qquad (4\text{-}16)$$

which gives the terrestrial radiative loss at the surface with clear skies above.

In addition, only a simple programming alteration is required to include the CO_2 modifications to recover the flux divergences $F_6^* - F_{10}^*$ and $F_2^* - F_6^*$ necessary for the computation of the layer temperature-change rates, Eqs. 4-1, 4-2.

4(b) Modification of net-flux F^* with cloudy skies.

As before, the cloud-cover amount CL is given by Eq. 2-9. Section 4(a) has dealt with the clear-sky fraction (1-CL) over gridpoint (i,j), and the remaining fraction CL therefore represents an overcast (extending vertically from $\sigma = .8$ to $\sigma = .4$) over the remainder of the grid area. As before, we are interested in F_{10}^*, F_6^*, F_2^* (but with overcast) over the gridpoint. The relevant schematic flux diagrams, after Yamamoto (1952), are depicted in Fig. 4. In Fig. 4, all emissivities are based upon the function ϵ_{WC} as computed using Eqs. 4-4 and 4-14 in proper combination of absorber masses relative to the reference level.

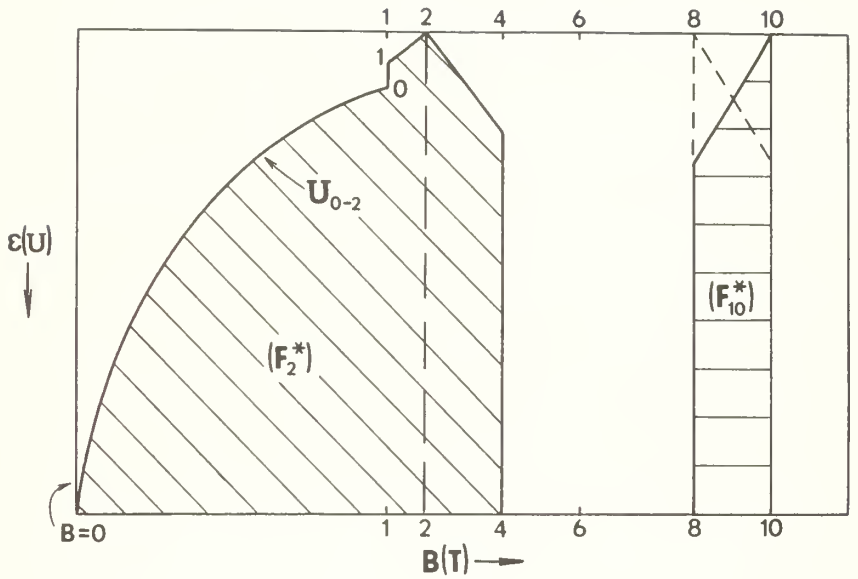

Fig. 4. Schematic area-depictions of net flux at reference levels 10 and 2, when an overcast cloud extends between levels 8 and 4 in the vertical. The horizontally-hatched area is F_{10}^*; the slant-hatched area is F_2^*. The net flux F_6^* is zero, since it lies within the black-body cloud. F_8^* is numerically equal to F_{10}^*.

4(b)A. Net flux F_{10}^{*} at earth, with overcast clouds.

The result for this case is based upon Fig. 4 and is given by the horizontally-hatched area:

$$F_{10}^{*} = (B_{10} - B_8)[1 - .5\ \epsilon_{WC}(U_{8-10}, C_{8-10})] \tag{4-17}$$

This is a cooling-rate at the earth-surface.

At the same time the net flux at level 8 (= the overcast-base) is an identically equal magnitude, so that the layer 8-10 is in radiative equilibrium. However, the cloud base receives net flux warming exactly equal to F_{10}^{*}, i.e.,

$$F_8^{*} = -F_{10}^{*}\ , \text{ a warming} \tag{4-18}$$

4(b)B. Net flux at level 6.

Since a layer of approximately 50 meters of average cloud-drop content may be regarded as a black body (Brunt, 1939) at the mean temperature of the cloud layer, it follows that level 6 is characterized by

$$F_6^{*} = 0 \tag{4-19}$$

4(b)C. Net flux at level 2.

The design of the result in this case is suggested by Fig. 4. Thus F_2^{*} becomes

$$F_2^{*} = B_4 - .5\Big\{\epsilon_{WC}(2\text{-}4)(B_4 - B_2) + \epsilon_{WC}(1\text{-}2)(B_2 - B_1) + 2B_1\Big[\frac{4.0\bar{\epsilon}(U_{0-2}, T_1)}{.353\ \log_{10} U_{0,2} + 3.56} + \Delta\epsilon_{WC}(U_{0,2}\ C_{0,2})\ \text{of (4-14)}\Big]\Big\} \tag{4-20}$$

after application of Eqs. 4-11, 4-12 to the truncated area of Fig. 4. This net flux is a much smaller value than that of Fig. 3C because of the cold black body interposed at level 4. The reduced net flux due to clouds is an effect often referred to as "cloud-contamination" in problems of remote sensing of the atmosphere.

4(c) Terrestrial radiative cooling rates in key atmospheric layers

(i) Upper layer (2,6)

The radiative flux divergence in the cloud-covered case is

$$(F_2^* \text{ of } 4\text{-}20) - F_6^* (= 0) \qquad (4\text{-}21)$$

This result, appropriately cloud-weighted with the clear sky result $F_2^* - F_6^*$ of Section 4(a), then gives the terrestrial radiative cooling in the layer (2,6). The cloud-weighted $F_2^* - F_6^*$ may then be used in connection with Eq. 4-2 to yield a temperature-change rate due to terrestrial radiation. The latter may then be combined with the insolational absorption of 3-29 to obtain an overall radiative change in the layer.

(ii) Lower layer (6,10)

The corresponding result for this cloud-covered layer is

$$(F_6^* = 0) - F_8^* = F_8^* = - F_{10}^* \qquad (4\text{-}22)$$

where a negative result indicates a net flux-convergence, or a warming rate. The result of (4-22) covers the layer (6,8). To this may be added the zero-change in layer (8,10), so that

$$F_6^* - F_{10}^* = - F_{10}^* \quad \text{of (4-17)} \qquad (4\text{-}23)$$

(iii) The interface level $\sigma = 1.0$

The terrestrial radiative transfer across the earth-surface is F_{10}^* which must now be cloud-weighted in the usual manner, i.e.

$$F_{10}^*(i,j) = CL[F_{10}^* \text{ of (4-17)}] + (1\text{-}CL)\ [F_{10}^* \text{ of (4-16)}] \qquad (4\text{-}24)$$

5. Maintenance of the heat budget

5(a) In the atmosphere

At each of the odd levels in Fig. 1, the diabatic heat-sources of the radiative type discussed in Sections 3 and 4 are included in the thermodynamic equation

$$\frac{\partial}{\partial t}(\pi C_p T_k) + \nabla \cdot (\pi C_p T_k \vec{V}_k) + \frac{\partial}{\partial \sigma}(\pi C_p T_k \dot{\sigma}_k) = \pi \dot{Q}_k$$

Here $\dot{Q}_k$ is the diabatic heating (cooling) rate per gram at level k including that due to radiation. $\dot{Q}_k$ should also include the latent heat released at level k at time-step t. The subject of latent-heat release and more generally of the atmospheric water vapor balance is not included in this paper.

5(b) At the earth's surface

The earth's surface is considered to be a heat reservoir of zero heat capacity over land, and of infinite heat capacity (a perfect insulator) over the ocean. The case of a solid ice sheet may be considered to be a predictable compromise between the land versus ocean cases. These earth-surface vertical heat-flow requirements lead to the following surface boundary conditions, essentially after Langlois and Kwok (1969) henceforth abbreviated to LK.

5(b)A. Over land

The external radiative surplus (deficit) at level 10 is

$$I_{10} - F_{10}^{*}$$

With the land surface considered to be of zero heat capacity, this surplus must be diffused upward in the form of sensible-heat conduction Γ and latent heat of evaporation E at the earth surface, across land:

$$I_{10} - F_{10}^{*} = \Gamma + E = \Gamma \left[1 + \frac{1}{r}\right] \qquad (5\text{-}1)$$

In (5-1), $r \equiv \Gamma/E$ is the so-called Bowen ratio, given empirically by Sellers as

$$r = 9.6(\sin \varphi)^2 - 7.93 \ (\sin \varphi) + 2.0 \qquad (5\text{-}2)$$

$$\sin \varphi \geq 0.4 \text{ for all } \varphi$$

In this treatment, a direct formulation of E over land is not achieved; rather, only an indirect computation making use of $E = \Gamma/r$ is employed.

The determination of the sensible-heat flux Γ is based upon its large-scale parameterization [(after Deardorff 1966), LK(1969)], and a simultaneous micrometeorological parameterization. Thus LK give the large-scale parameterization as

$$\Gamma = -\rho_{10} C_p \ K \frac{\Delta\theta}{\Delta Z}$$

$$\Gamma = \rho_{10} C_p \left(\frac{K^*}{1 + \dfrac{a^*(\theta_9 - \theta_S)}{Z_9 - Z_{10}}}\right)\left\{\gamma_C - \frac{\theta_9 - \theta_x}{Z_9 - Z_{10}}\right\} \qquad (5\text{-}3)$$

and the micrometeorological equivalent as

$$\Gamma = \rho_{10} C_p C_D V_S (T_g - T_x) \qquad (5\text{-}4)$$

In (5-4), V_S is related to the surface geostrophic wind through $V_S = .8|V_{go}| + 2.2$ in mps. In (5-3) K^*, a^* and γ_C are turbulent-transfer coefficients whose values have recently been documented by Kaitala (1972). The value of θ_S is related to the estimated $T_{10} = T_S$ by

$$\theta_S = T_{10}\left(\frac{\pi}{1000}\right)^{.286} \qquad (5\text{-}5)$$

where $T_g - T_x$ is the actual temperature lapse (compatible with Eq. 5-3) within the constant flux boundary layer.

A(i) Overland boundary adjustment of surface temperature

The combination of Eqs 5-3, 5-4 leads to the solution for T_x at the top of the boundary layer:

$$T_x = \frac{(Z_9 - Z_{10})[C_D V_S T_g - K\gamma_C] + K\,\theta_9}{[K(\frac{1000}{\pi})^{.286} + C_D V_S (Z_9 - Z_{10})]} \qquad (5\text{-}6)$$

In (5-6) θ_9 is related to T_9 by a formula of form (5-5). If one starts over land with $T_g = T_S$, a solution for T_x emerges and a value of Γ is available from (5-4). Application of the Bowen-ratio technique then provides a value of E. With first iterates of Γ and E available for use in (5-1), an adjustment in surface temperature T_{10} is achieved as follows

$$F_{10}^{*}(T_g) = I_{10} - \Gamma(1 + \frac{1}{r}) \qquad (5\text{-}7)$$

$$F_{10}^{*}(T_g) = B_{10} - F_d = F_{10}^{*}(T_S) + (\frac{\partial B}{\partial T})_{T_S}(T_g - T_S) \qquad (5\text{-}8)$$

If one makes use of Eqs 5-7, 5-8 for correction of Γ in 5-6, a revised Γ of (5-5) results and sequentially there is a second iterate T_{g2} from 5-7, 5-8. This process must converge rapidly in view of the large coefficient $4\,T_S^{3}$ or $4\,T_{g1}^{3}$, depending upon the step in the iteration procedure. When the several iterative steps are complete, a heat balance exists at the earth's (land) surface, which has realistically determined the surface temperature. Induced changes in F_6^{*} and F_2^{*} have resulted from the recalculation of the earth-surface temperature to be T_g(instead of T_S). These become, respectively, in the case of clear-skies

$$\Delta F_6^{*} = [B(T_{gn}) - B(T_S)]\,[1 - \epsilon_{WC}(6\text{-}10)] \qquad (5\text{-}9)$$

$$\Delta F_2^{*} = [B(T_{gn}) - B(T_S)]\,[1 - \epsilon_{WC}(2\text{-}10)] \qquad (5\text{-}10)$$

where n is the iterate-step and ϵ_{WC} is given by Eqs, (4-4, 4-14)

With overcast skies only the minor correction below applicable in the layer (8,10) occurs

$$\Delta F^{*}(8,10) = [B(T_g) - B(T_S)]\,[1 - \epsilon_{WC}(U_{8,10})] \qquad (5\text{-}11)$$

A(ii) Over the ice-free ocean.

Here it is assumed that Eqs 5-5, 5-6 still apply, but that T_g is known from the sea-surface analysis, which is held constant during the prediction process. In this case, a unique value of T_x and therefore of Γ results. It is no longer necessary to make the Bowen ratio assumption for the surface-layer evaporative heat-transfer rate. Instead the analog of (5-3) is formed

$$E = L\rho_{10} \frac{K^*}{1 + a^*\left(\frac{\theta_9 - \theta_S}{Z_9 - Z_{10}}\right)} \frac{q_x - q_9}{Z_9 - Z_{10}} \tag{5-12}$$

and is coupled with the analog of (5-4)

$$E = L\rho_{10} C_D V_S (q_{Sg} - q_x) \tag{5-13}$$

Eqs. 5-12, 5-13 yield the result

$$q_x = \frac{Kq_9 + (Z_9 - Z_{10})\, C_D V_S q_{Sg}}{K + (Z_9 - Z_{10})\, C_D V_S} \tag{5-14}$$

with

$$q_{Sg} = \frac{.622\, e^{(AE - BE/T_g)}}{\pi - e^{(AE - BE/T_g)}} \tag{5-15}$$

AE = 21.656; BE = 5418. The last relationship is the Clausius-Clapeyron equation.

In this case (5-1) may be rewritten

$$F_{10}^* = I_{10} - (E + \Gamma) \tag{5-16}$$

If F_{10}^* of (5-16) differs from that computed using Eq. (4-16), the difference $I_{10} - F_{10}^*$ should be used to increment both E and Γ in the relative proportion of the magnitudes of the latter pair.

A(iii) Over ice-covered ocean

In this case, the surface-to-air boundary condition may be stated as

$$\Gamma = I_{10} - F_{10}^{*} - b(T_W - T_g) \tag{5-17}$$

where b = ice-conduction coefficient (697.8 erg $cm^{-2} sec^{-1} deg^{-1}$)

T_w = 271.2K is the freezing point of sea water

T_g = the desired temperature at the ice-air interface

The evaporative-heat transfer E has been omitted from 5-17. However, Eqs. 5-3, 5-4 are still valid and it is still necessary to obtain T_x in order to evaluate Γ by 5-4. Accepting $T_g = T_S$ as the first iterate, it is possible to adjust $F_{10}^{*}(T_g)$ of (5-17) as was done in Eq. 5-8. If only a single iteration is required, an analytic formula for T_x results [Kaitala (1972); LK(1969)], namely:

$$T_x = \frac{\zeta D + \dfrac{\beta\theta_9}{Z_9 - Z_{10}} - \beta\gamma_C}{\dfrac{\beta}{Z_9 - Z_S}\left(\dfrac{1000}{.9\pi}\right)^{.286} + \rho_{10} C_p C_D V_S (1-\zeta)} \tag{5-18}$$

where

$$D = I_{10} + bT_w + 4St^{*}T_S^{4} - F_{10}^{*}(T_S)$$

$$\beta = \rho_{10} C_p \frac{K^{*}}{\left[1 + a^{*}\dfrac{(\theta_9 - \theta_S)}{Z_9 - Z_S}\right]}$$

$$\zeta = C_T/(C_T + b + 4St^{*}T_S^{3})$$

$$C_T = \rho_{10} C_p C_D V_S \tag{5-19}$$

With T_x known in terms of T_g, one may iterate successively upon the values of the latter using 5-8 and obtain convergent values of T_g as well as of the sensible heat transport Γ. With T_S replaced by a more realistic value, T_g, it is relevant again to replace

$$F_6^* \text{ by } F_6^*(T_g)$$

$$F_2^* \text{ by } F_2^*(T_g)$$

$$F_{10}^* \text{by } F_{10}^*(T_g)$$

following the method of Eqs. 5-9, 5-10.

APPENDIX A

Vertical extrapolation of the mixing ratio profile.

When London's (1957) climatological soundings included mixing ratios $q(p)$ to levels of $p = 0.3\pi$, the interpolated values of $q(\sigma)$(where 10.0σ = 9., 7., 5., 3.) were subjected to a best-fit against pressure in the logarithmic form

$$\ln \frac{q(\sigma)}{q_5} = \lambda \ln \frac{p}{p_5} = \lambda \ln \frac{\sigma}{.5} \qquad \text{(A-1)}$$

Eq. (A-1) was tested for eight latitude belts on the Northern Hemisphere and over four seasonal mean-soundings at each belt. The parameter λ is related to the correlation coefficient $r(Y,X)$(where $Y = \ln q/q_5$ and $X = \ln p/p_5$), which was well in excess of $r \geq 0.99$ in each sounding. This indicated an effective method of extrapolation in the form

$$\frac{q}{q_5} = \left(\frac{p}{p_5}\right)^{\lambda} \qquad \text{(A-2)}$$

as also suggested by Smith (1966). This relationship permitted extrapolation of individual moisture soundings to $p = .3\pi$ when $q(p)$ values existed at $p = .9\pi$, $.7\pi$, $.5\pi$ at analysis points.

When moisture values $q(p)$ exist also at $p = .1\pi$, a relationship of form (A-1) was also found to give close verification at $\sigma = 0.1\pi$ in terms of a best-fit power law

$$\frac{q}{q_3} = \left(\frac{p}{p_3}\right)^{\lambda} \qquad \text{(A-3)}$$

with λ determined using the four pairs of $(q/q_3,\ p/p_3)$ values from the analysis covering each gridpoint.

APPENDIX B

Solar undepleted insolation in spherical coordinates.

The incoming undepleted insolation is given by

$$F = S[\sin \varphi \sin \delta + \cos \varphi \cos \delta \cos h] \left(\frac{r}{r_m}\right)^{-2} \qquad \text{(B-1)}$$

where (r/r_m) is listed by Julian date in the Smithsonian Tables (List, 1963) number 169. Likewise, the declination δ is listed in that same source, but may also be computed from

$$\sin \delta = .39785 \sin[4.88578 + .0172D + .03342 \sin(.0172D)$$
$$-.001388 \cos(.0172D) + .000348 \sin(.0344D) -.000028 \cos(.0344D)] \qquad \text{(B-2)}$$

The hour angle h on day D is given in terms of GMT (denoted by Z) by means of the relationships

$$t = \text{MOD}\left[\left(Z + \frac{\lambda}{2\pi/24}\right) + 24,\ 24\right]$$
$$\cos h(Z,\lambda) = \cos \left[\frac{2\pi}{24} (t-6) - \frac{\pi}{2}\right] \qquad \text{(B-3)}$$

The expression in brackets in (B-1) is cos θ, where θ is solar zenith angle at latitude φ, δ and hour angle h, the latter given by B-3. If cos θ of (B-1) becomes negative, it is set to zero.

APPENDIX C

Determination of the absorber-equivalent water vapor mass U_c for droplet-absorption in clouds

In clouds, the water droplet-absorption has been modeled using the diffuse-path absorptivity of Manabe-Moller (cf., a_{CLD} of 3-23). In this paper the value of a_{CLD}, due solely to cloud droplets has been taken after theoretical computations of Korb, Michalowski and Moller (1956), and subsequently used also by Manabe and Strickler (1964). These values are as listed below in Table 4.

Table 4. Absorptivities (a_{CLD}) of cloud droplets

Cloud-type	a_{CLD}	R_c	Equivalent Lat. band
Low	.035	.21	0-39N
Middle	.020	.48	40-64N
High	.005	.69	65-90N

Since only a single cloud-layer has been invoked in the radiative model presented here, the larger absorptivities associated with low clouds (largest droplets) have been associated with an equivalent latitude band 0-39N; while intermediate values of a_{CLD} have been identified with an intermediate latitude band, 40-64N. Finally, the minimum value a_{CLD} has been ascribed to the latitude band 65-90N. The values a_{CLD} of Table 4 are due solely to absorption by either the liquid-water or the solid-ice content, depending upon the cloud type considered. The values a_{CLD} of Table 4 are then to be considered absorption-means for the latitude belts under consideration. No specific use has been made of the values of R_c, although it seems reasonable to ascribe these reflectivity values to the same latitude bands for which a_{CLD}-values are proposed in Table 4.

The absorptivities of Table 4 apply over the full energy range of the solar spectrum. If cloud-water absorptivities are to be modeled as water-vapor equivalents occurring solely in the F_A-wavelengths, then each value of a_{CLD} must be multiplied by (1./.349) on the left side of (3-23). Thus one obtains the water vapor equivalent of the cloud-water absorptivity in the form

$$a^* \equiv 2.8653 a_{CLD} = \left\{[\tfrac{5}{3}(U_{4,8} + U_c)]^{.303} - [\tfrac{5}{3}U_{4,8}]^{.303}\right\}(.271) \qquad \text{(C-1)}$$

using a Manabe-Möller parameterization similar to (3-23). In (C-1), the absorption in clouds has been spread over the full cloud-depth which contains $U_{4,8}$, a known absorber mass of water vapor as determined from the sounding. Eq. C-1 may be solved for $U_c/U_{4,8}$ using the appropriate value of $a^* = 2.8653 a_{CLD}$ and Table 4. The desired solution assumes the form

$$(1 + \frac{U_c}{U_{4,8}})^{.303} = 1 + \frac{a^*}{.271}\,(\frac{3/5}{U_{4,8}})^{.303}$$

which becomes

$$\frac{U_c}{U_{4,8}} = \left\{[1 + \frac{a^*}{.271}\,(\frac{.6}{U_{4,8}})^{.303}]^{\frac{1}{.303}} - 1\right\} \qquad \text{(C-2)}$$

where the exponent $1/0.303 = 3.3003$

A graphical solution of (C-2) for U_c as a function of $U_{4,8}$ is presented in Table 5 as a^* varies over the low, middle and high cloud (i.e. latitude) types of Table 4.

$U_{4,8}$	$U_c(1)$	$U_c(2)$	$U_c(3)$
0.01	0.14170	0.05118	0.00740
0.02	0.18936	0.07292	0.01155
0.05	0.28686	0.12003	0.02103
0.10	0.40852	0.17651	0.03329
0.15	0.50529	0.22673	0.04365
0.20	0.58995	0.26939	0.05294
0.30	0.73785	0.34473	0.06955
0.50	0.98617	0.47287	0.09826
0.80	1.29740	0.63548	0.13520
1.00	1.48119	0.73226	0.15739
1.20	1.65219	0.82271	0.17822
1.40	1.81232	0.90822	0.19800
1.60	1.96648	0.98974	0.21691
1.80	2.11306	1.06793	0.23510
2.00	2.25403	1.14331	0.25267
2.20	2.39016	1.21623	0.26970
2.40	2.52206	1.28699	0.28626
2.60	2.65022	1.35584	0.30240
2.80	2.77499	1.42297	0.31816
3.00	2.89675	1.48854	0.33357

Table 5. Water-vapor equivalent U_c for droplet absorption in relation to the pressure-scaled water-vapor absorber mass $U_{4,8}$ (in the sounding layer (4,8)). Case $U_c(1)$ corresponds to low-cloud water-drop absorptivity; $U_c(2)$ to mid-level cloud-drop absorptivity; $U_c(3)$ to high-cloud absorptivity.

REFERENCES

Arakawa, A., A. Katayama and Y. Mintz, 1968: Numerical simulation of the general circulation of the atmosphere. Proceedings of the WMO/IUGG Symposium on Numerical Weather Prediction, Tokyo, 1968, pp. IV-7 to IV-8-12.

Brunt, D., 1939: Physical and dynamical meteorology, Cambridge University, London, 428 pp.

Coulson, K. L., 1959: Radiative flux from the top of a Rayleigh atmosphere. Ph.D. dissertation, Department of Meteorology, University of California, Los Angeles, pp. 60.

Deardorff, J. W., 1966: The counter-gradient heat flux in the lower atmosphere and in the laboratory. Journal of the Atmospheric Sciences, Vol. 23, No. 5, pp. 503-506.

Gates, W. L., E. S. Batten, A. B. Kahle and A. B. Nelson, 1971: A documentation of the Mintz-Arakawa two-level atmospheric circulation model. Advance Research Projects Agency Report No. R-877-ARPA, Rand Corporation,Santa Monica, Calif., 408 pp.

Joseph, J. H., 1966: Calculation of radiative heating in numerical general circulation models. Tech. Rpt. No. 1, Dept. of Meteorology, University, Los Angeles, pp. 60.

Kaitala, J., 1972: Heating and moisture source terms. Manuscript documenting heating terms in the Fleet Numerical Weather Central operational primitive-equation model, pp. 18.

Katayama, A., 1966: On the radiation budget of the troposphere over the northern hemisphere (I). Journal of the Meteorological Society of Japan, vol. 44, No. 6, pp. 381-401.

Kesel, P. G. and F. J. Winninghoff, 1972: The Fleet Numerical Weather Central operational primitive-equation model, Monthly Weather Review, vol. 100, no. 5, pp. 360-373.

Korb, G., J. Michalowsky and F. Moller, 1956: Investigation on the heat balance of the troposphere. Tech. Rept No. 1, Contract AF61(514) -863. 94pp. (OTS No. PB127016, Obtainable from Library of Congress).

Langlois, W. E. and H. C. W. Kwok, 1969: Description of the Mintz-Arakawa numerical general circulation model. Numerical Simulation of Weather and Climate Tech. Rpt. No. 3, Dept. of Meteorology, University of California.

London, J., 1957: A study of the atmospheric heat balance. College of Engineering, New York University. Final report on AFCRL contract 19(122)-165, also issued as AFCRC-TR-57-287.

Manabe, S. and F. Moller , 1961: On the radiative equilibrium and heat balance of the atmosphere. Monthly Weather Review, vol. 89, no. 12, pp. 503-522.

Manabe, S. and R. F. Strickler, 1964: Thermal equilibrium of the atmosphere with convective adjustment. Journal of the Atmospheric Sciences, vol. 12, no. 4, pp. 361-385.

Möller, F. and E. Rashke, 1964: Evaluation of TIROS III radiation data. National Aeronautics and Space Administration Contractor Report, NASA CR-112, Washington, D. C., 114 pp.

Oliger, J. E., R. E. Wellck, A. Kasahara and W. M. Washington, 1970: Description of the NCAR global circulation model. Tech. note STR-56, National Center for Atmospheric Research, Boulder, Colo., 94 pp.

Posey, J. W. and P. F. Clapp, 1964: Global distribution of normal surface albedo. Geophisica International, Mexico City, pp. 33-48.

Sasamori, T., 1968: , The radiative cooling calculation for application to general circulation experiments. Journal of Applied Meteorology, vol. 7, no. 5, pp. 721-729.

Smagorinsky, J., 1960: On the dynamical prediction of large-scale condensation by numerical methods. Geophysical Monograph, No. 5, American Geophysical Union, Washington, D. C., pp. 71-78.

Smith, W. L., 1966: Note on the relationship between total precipitable water and surface dew point. Journal of Applied Meteorology, vol. 5, no. 6, pp. 726-727.

Yamamoto, G., 1952: On a radiation chart. Sci. Repts. of the Tohoku Univ., Series No. 4, pp. 9-23.

DISTRIBUTION LIST

	No. Copies
Defense Documentation Center Cameron Station Alexandria, Virginia 22314	12
Officer-in-Charge Environmental Prediction Research Facility Naval Postgraduate School Monterey, California 93940	5
Commanding Officer Naval Weather Service Command 3101 Building 200 Washington Navy Yard Washington, D.C. 20390	1
Commanding Officer Fleet Numerical Weather Central Monterey, California 93940	5
Library, Code 0212 Naval Postgraduate School Monterey, California 93940	2
Dean of Research Administration, Code 023 Naval Postgraduate School Monterey, California 93940	2
Department of Meteorology Reference Center Naval Postgraduate School Monterey, California 93940	1
Professor G. J. Haltiner Department of Meteorology, Code 51 Naval Postgraduate School Monterey, California 93940	2
Professor R. T. Williams, Code 51Wu Naval Postgraduate School Monterey, California 93940	1
Professor F. L. Martin, Code 51Mr Naval Postgraduate School Monterey, California 93940	12

Security Classification

DOCUMENT CONTROL DATA - R & D

(Security classification of title, body of abstract and indexing annotation must be entered when the overall report is classified)

1. ORIGINATING ACTIVITY *(Corporate author)*

Naval Postgraduate School
Monterey, California 93940

2a. REPORT SECURITY CLASSIFICATION

Unclassified

2b. GROUP

3. REPORT TITLE

Description of a Radiation Package for the
Naval Postgraduate School General Circulation Model

4. DESCRIPTIVE NOTES *(Type of report and, inclusive dates)*

Technical Report, 1 December 1972

5. AUTHOR(S) *(First name, middle initial, last name)*

Frank L. Martin

6. REPORT DATE	7a. TOTAL NO. OF PAGES	7b. NO. OF REFS
1 December 1972	51	21

8a. CONTRACT OR GRANT NO.	9a. ORIGINATOR'S REPORT NUMBER(S)
b. PROJECT NO.	
c.	9b. OTHER REPORT NO(S) *(Any other numbers that may be assigned this report)*
d.	

10. DISTRIBUTION STATEMENT

Approved for public release; distribution unlimited.

11. SUPPLEMENTARY NOTES	12. SPONSORING MILITARY ACTIVITY
This research was partially supported by Environmental Prediction and Research Facility, Monterey, Calif.	Naval Postgraduate School Monterey, California 93940

13. ABSTRACT

A method has been devised for integrating the pressure-scaled water-vapor and CO_2 absorber masses from the surface to the σ - levels used for prediction in the Naval Postgraduate School primitive equation model. Using empirical expressions for atmospheric absorptivity, scattering-reflectivity, cloud-reflectivity and earth-surface reflectivity, the useful solar insolations absorbed at earth and in the key atmospheric layers above the earth have been formulated. The terrestrial cooling effect at earth and in these same key atmospheric layers have also been formulated using recently published emissivities for the joint effects of water vapor and CO_2. As a result, the radiative heating (cooling) at key levels may be ascertained for input into the atmospheric thermodynamic equation. In addition, application of atmospheric boundary-layer modelling permits determination of the surface-layer turbulent transports (in the vertical) of sensible and latent heat at the earth's surface. These turbulent transports act in such a way as to provide a heat balance at the earth's surface.

14 KEY WORDS	LINK A		LINK B		LINK C	
	ROLE	WT	ROLE	WT	ROLE	WT
Pressure-scaled absorber masses						
Insolation						
Manabe-Moller absorption						
Flux-emissivity of water vapor and CO_2						
Black-body flux						
Surface boundary conditions						
Primitive equation prediction model						
σ-level surfaces						
Diabatic heating						